

To be published in Optics Letters:

Title: Real-time quantitative phase reconstruction in off-axis digital holography using multiplexing

Authors: Pinhas Girshovitz and Natan Shaked

Accepted: 4 March 2014

Posted: 4 March 2014

Doc. ID: 205370

Published by

OSA

Real-time quantitative phase reconstruction in off-axis digital holography using multiplexing

Pinhas Girshovitz and Natan T. Shaked*

Department of Biomedical Engineering, Faculty of Engineering, Tel-Aviv University, Tel-Aviv 69978, Israel.

*Corresponding author: nshaked@tau.ac.il

Received Month X, XXXX; revised Month X, XXXX; accepted Month X, XXXX; posted Month X, XXXX (Doc. ID XXXXX); published Month X, XXXX

We present a new approach for obtaining significant speedup in the digital processing of extracting unwrapped phase profiles from off-axis digital holograms. The new technique digitally multiplexes two orthogonal off-axis holograms, where the digital reconstruction, including spatial filtering and two-dimensional phase unwrapping on decreased number of pixels, can be performed on both holograms together, without redundant operations. Using this technique, we were able to reconstruct, for the first time to our knowledge, off-axis holograms with 1 megapixel in more than 30 frames per second using a standard single-core personal computer on a Matlab platform, without using a graphic processing-unit programming or parallel computing. This new technique is important for real-time quantitative visualization and measurements of highly dynamic samples, and is applicable for a wide range of applications, including rapid biological cell imaging and real-time nondestructive testing. After comparing the speedups obtained by the new technique for holograms of various sizes, we present experimental results of real-time quantitative phase visualization of cells flowing rapidly through a micro-channel.

OCIS Codes: 120.3180, 090.1995, 090.4220, 110.3175, 100.5070, 100.5088.

Digital holography is capable of capturing the complex wave front (amplitude and phase) of the light interacted with an object by using a digital camera. This is obtained by recording the interference pattern between two mutually coherent waves, a sample wave, which interacts with the sample, and a reference wave. In off-axis holography, there is a small angle between the sample and reference waves, which allows reconstruction of the complex wave front from a single camera exposure. The retrieved phase profile is proportional the optical thickness of the sample, where the accuracy of the measurement can be sub-nanometric [1]. Due to its unique advantages, off-axis digital holography found many applications, including label-free imaging of live biological cells, and nondestructive quantitative quality tests and metrology in ambient conditions [2].

The scan-free, single-exposure nature of off-axis holography allows quantitative recording of very fast dynamic samples, limited only by the true frame rate of the camera. After acquisition, the digital processing of the hologram to the quantitative phase profile mainly includes digital spatial filtering and phase unwrapping [1]. Due to limited computational resources, standard personal computers can typically process two holograms of 1 megapixel in a second. Therefore, this processing is typically done off-line, after the acquisition of the dynamic process is already done. Simultaneous processing of the phase profiles during the acquisition of the holograms is highly advantageous for real-time visualization, such as for controlling a dynamic process during its holographic imaging or for rapid medical diagnosis.

In order to allow faster digital processing in off-axis holography, recent works suggest using the multiple microprocessors of the computer's graphic processing unit (GPU), which allows processing of holograms of 1 megapixel in more than a video rate [3,4]. Using GPU processing, however, requires

special graphic cards and high programming capabilities.

In this Letter, we present a new approach for rapid reconstruction of unwrapped phase profiles from off-axis holograms. We show that even when implemented on a simple single-core personal computer, without the help of the GPU, we can obtain more than video rate when processing 1 megapixel holograms. The new algorithmic approach significantly reduces redundant calculations done in the conventional Fourier-based algorithm, making the reconstruction process more efficient. The presented algorithms do not limit the samples that can be imaged, or require advanced hardware to enable parallelized processing. Still, they are able to reconstruct the unwrapped phase profile much faster than it has been possible until now, and without losing image quality.

Assuming straight vertical fringes, the recorded off-axis image hologram can be mathematically expressed as follows [1]:

$$\begin{aligned} H &= |E_s + E_r|^2 = |E_s|^2 + |E_r|^2 + E_s^* E_r + E_s E_r^* \\ &= I_{r+s} + 2|E_s||E_r| \cos\left(\frac{2\pi}{\lambda} [OPD + y \sin(\theta)]\right), \end{aligned} \quad (1)$$

where E_s and E_r are the sample and reference complex waves, respectively, I_{r+s} represents the intensities of sample and reference beams, OPD is the total optical path delay or optical thickness of the sample, λ is the illumination wavelength, and θ is the angle between the sample and reference waves in relation to the y axis. Per camera, we assume a maximal angle θ to allow best location of the cross-correlations in the spatial-frequency domain, which allows complete separation of $E_s E_r^*$ from Eq. (1) [5].

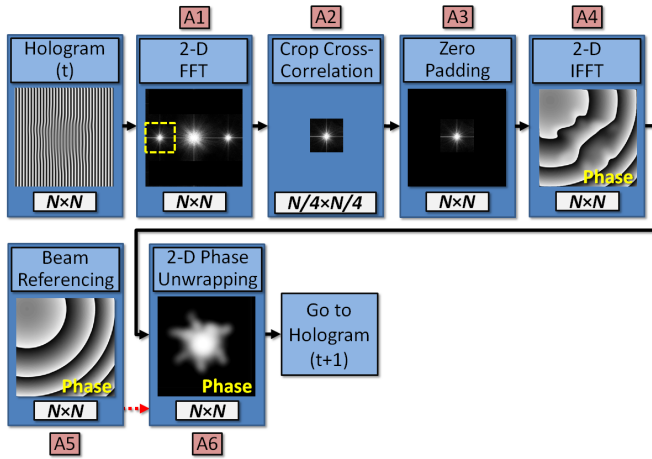


Fig. 1. Algorithm A: conventional algorithm for extracting quantitative phase profiles from off-axis holograms.

The conventional digital process for extracting the unwrapped phase profile from an off-axis image hologram is presented in Fig. 1. This algorithm, named Algorithm A, includes the following steps:

- A1. Two-dimensional (2-D) fast Fourier transform (FFT): Convert the digital hologram, containing $N \times N$ real pixels, to the spatial-frequency domain using a 2-D FFT, which results in a matrix containing $N \times N$ complex pixels.
- A2. Cross-correlation cropping: Crop the $N/4 \times N/4$ cross-correlation (yellow square in Fig. 1). In an efficient system, the entire wave-front spatial-frequency content occupies $N/4 \times N/4$ pixels [5].
- A3. Zero padding: Insert the cropped cross-correlation to the center of an empty matrix containing $N \times N$ pixels.
- A4. 2-D inverse FFT (IFFT): Convert the zero-padded cross-correlation back to the image domain using a 2-D IFFT, resulting in an $N \times N$ complex matrix representing the sample wave front.
- A5. Beam referencing: To compensate for stationary aberrations and curvatures in the beam profile, before the experiment, acquire a hologram without the sample, and process it into the sample-free wave front using steps A1-A4 above. Then, divide the sample wave front from step A4 by the sample-free wave front.
- A6. Phase unwrapping: The argument of the resulting $N \times N$ complex matrix is the wrapped phase, and it is subjected to 2π ambiguities in cases that the optical thickness is larger than the illumination wavelength. In these cases, we apply a 2-D phase unwrapping algorithm, and obtain an $N \times N$ matrix representing the unwrapped phase, free of 2π ambiguities.

Although good selection of the unwrapping algorithm can help speed up the processing, in general, 2-D unwrapping algorithms are slow, since they scan the wrapped phase matrix and look where the spatial phase gradients contain unreasonable

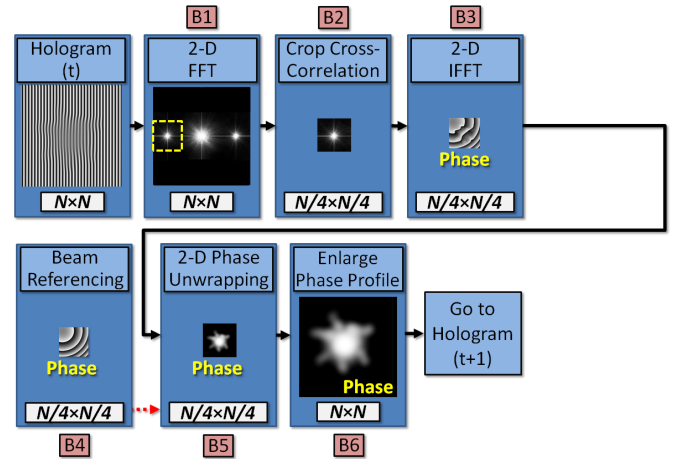


Fig. 2. Algorithm B: Cropped cross-correlation algorithm for extracting quantitative phase profiles from off-axis holograms.

2π jumps. Decreasing the number of pixels in the wrapped phase matrix will significantly speed up the unwrapping process. In fact, after cropping the cross-correlation term in step A2 above, there is no need to return to a matrix equals in size to the original image ($N \times N$), and it is enough to continue working with the cropped matrix containing only $N/4 \times N/4$ pixels. Thus, the zero padding in step A3 causes redundant calculations in the 2-D IFFT (step A4), in the beam referencing (step A5) and, especially, in the 2-D phase unwrapping (step A6). If we skip step A3, we will work on a matrix which is 16 times smaller. Only at the end of the process, the unwrapped phase profile can be enlarged back from $N/4 \times N/4$ pixels to $N \times N$ pixels. As will be experimentally demonstrated, this simple change spares significant amount of calculation time, but does not damage the quality of the resulting unwrapped phase profile. Figure 2 presents the above-described cropped cross-correlation algorithm, referred to as Algorithm B. This algorithm contains the following steps:

- B1. 2-D FFT: Same as step A1.
- B2. Cross-correlation cropping: Same as step A2.
- B3. 2-D IFFT: Convert the $N/4 \times N/4$ cropped cross-correlation back to the image domain by using a 2-D IFFT, resulting in an $N/4 \times N/4$ complex matrix representing the sample wave front.
- B4. Beam referencing: Before the experiment, calculate the $N/4 \times N/4$ sample-free wave front using steps B1-B3 above, and divide the sample wave front by the sample-free wave front.
- B5. Phase unwrapping: The argument of the resulting $N/4 \times N/4$ matrix is the wrapped phase. To solve 2π ambiguities, apply a 2-D phase unwrapping, which results in the $N/4 \times N/4$ unwrapped phase matrix.
- B6. Enlarge unwrapped phase profile: Enlarge the $N/4 \times N/4$ unwrapped phase matrix to the final $N \times N$ unwrapped phase matrix.

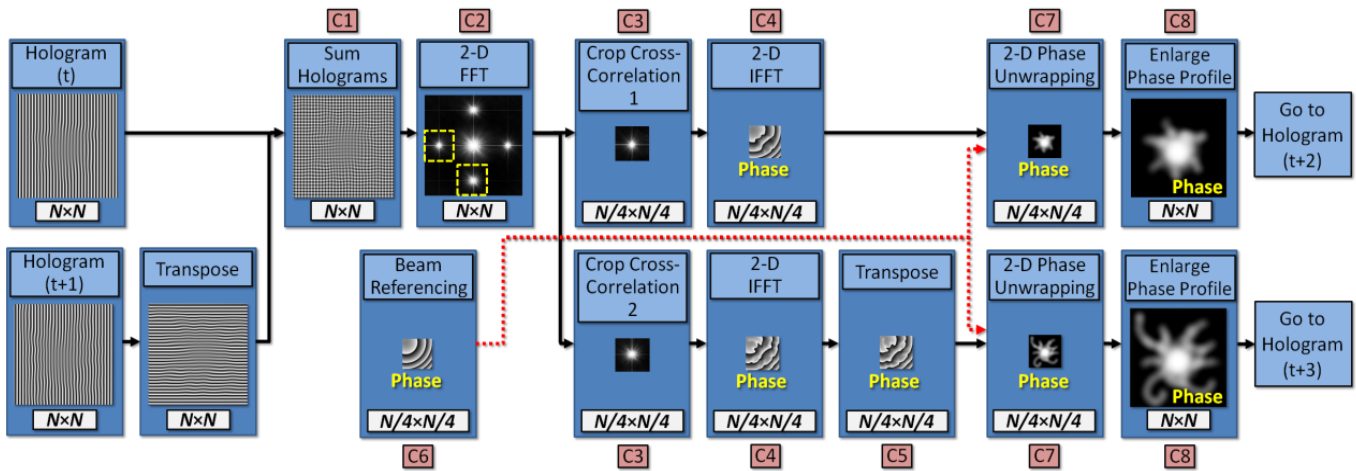


Fig. 3. Algorithm C: Hologram-multiplexing algorithm for extraction of the quantitative phase profile from off-axis holograms.

Although Algorithm B saves computation time from the point of cropping the cross-correlation (step B2) and forward, there is still a relatively slow Fourier transform in step B1. Therefore, we propose to exploit unnecessary calculations performed anyway by the 2-D FFT to calculate two sample wave fronts from a single multiplexed hologram.

Multiplexing of several off-axis holograms has been suggested previously [6], and optical multiplexing have been demonstrated [5]. In this Letter, we use digital hologram multiplexing, in the first time to our knowledge, to speed up the off-axis hologram reconstruction process.

Due to the off-axis holographic encoding, there is an empty space in the spatial-frequency domain (see the boxes of the 2-D FFT in Figs. 1 and 2), to which additional cross-correlations can be inserted. This is performed by taking the next hologram to be processed, rotating it in 90° (transposing is fast computational operation), so that the fringes of the second hologram will be orthogonal to the fringes of the first hologram. Summing the holograms yields a multiplexed hologram. Then, using a single 2-D FFT on the multiplexed hologram, we extract two distinct cross-correlations, each of which is originated from a different initial hologram. Then, we can process each of these two cropped cross-correlations without zero padding (like in Algorithm B), and rotate one of them before the beam referencing step. Figure 3 presents this hologram-multiplexing algorithm, referred to as Algorithm C, which contains the following steps:

- C1. Hologram multiplexing: Sum a hologram with a transverse (90° -rotated) version of the next hologram, which yields the multiplex hologram containing $N \times N$ pixels.
- C2. 2-D FFT: Same as steps A1 or B1.
- C3. Cross-correlation cropping $\times 2$: Crop the vertical cross-correlation and the horizontal cross-correlation, each containing $N/4 \times N/4$ pixels.
- C4. 2-D IFFT $\times 2$: Same as step B3, but for both the

horizontal and vertical cross-correlations. This results in two $N/4 \times N/4$ complex wave fronts.

- C5. Transposing: Rotate the complex wave front originated from vertical cross-correlation in 90° .
- C6. Beam referencing $\times 2$: Same as step B4, but for both wave fronts.
- C7. Phase unwrapping $\times 2$: Same as step B5, but for both wave fronts.
- C8. Enlarge unwrapped phase profile $\times 2$: Same as step B6, but for both wave fronts.

Note that steps C3-C8 can be implemented in parallel in case that more than one processing unit is available. It should also be noted that using a 2-D FFT on the multiplexed hologram is significantly more efficient than applying a 1-D FFT on two separate holograms with straight fringes, since in the latter case, the cross-correlation terms will contain $N \times N/4$ pixels, which will require more processing in the IFFT, the beam referencing, and the unwrapping steps.

To evaluate the algorithms, we acquired off-axis image holograms using a portable interferometric module connected to an inverted microscope and a CMOS digital camera (Thorlabs, DCC1545M) [7]. The processing was implemented on Matlab R2012b and Labview. We used a simple personal computer (Intel i7-2600, 3.4GHz CPU, 8GB RAM), without using GPU or parallel processing (only a single core was utilized). The 2D-SRNCP algorithm was used for phase unwrapping [8].

First, since Algorithms B and C work with cropped images, we verified on a phase 1951 USAF target, created by focused-ion-beam lithography on glass, that all algorithms yield comparable results, without loss in the optical system resolution (600 nm [7]). These results are shown in Fig. 4.

Next, we compared the average run times of the different algorithms and computational operations for a hologram containing 1024×1024 pixels, with 1200 repetitions. As shown in Table 1, the

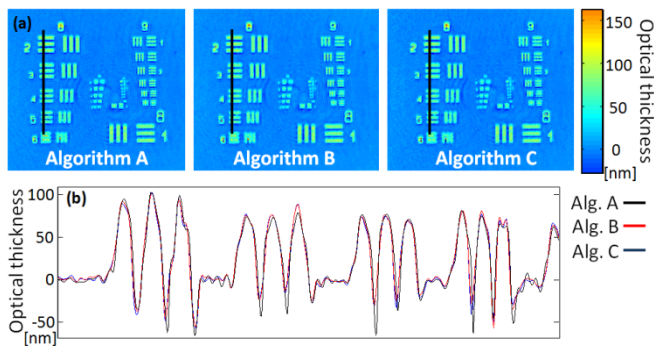


Fig. 4. (a) Phase reconstruction quality comparison for a phase 1951 USAF test target. (b) Cross sections along the black lines shown in (a). Alg. – Algorithm.

unwrapping in the conventional algorithm (A) consumes more than 90% of the total time due to running on a large phase profile. By using cropped images in Algorithms B and C, the unwrapping was performed 25 times faster and the 2-D IFFT was performed 9 times faster, enabling a significant decrease in the total calculation time. Also note that matrix transposing, summing and enlarging (included in the 'Others' column in Table 1) do not consume significant calculation time. The improvement between B and C is mostly due to the single 2-D FFT running on a multiplexed hologram containing two wave fronts, meaning that per one hologram, the FFT takes half the time. Overall, we obtained a speedup of 16 when comparing A and C.

We then examined the three algorithms on four data sets of 400 holograms, containing 1024×1024 , 768×768 , 512×512 , and 256×256 pixels each. Per combination, 10 runs were done. As shown in Fig. 5, there is an increase of up to 15.8 in the average

Table 1. Comparison between the *processing times* (msec) of a single hologram containing 1024×1024 pixels.

Alg*	FFT	IFFT	Unwrap	Others	Total
A	13.806	13.442	457.970	22.381	507.6
B	14.005	1.442	18.127	6.627	40.2
C	6.588	1.384	18.125	4.003	32.1

*Alg = Algorithm.

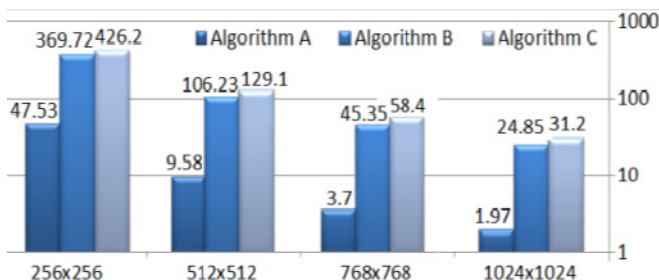


Fig. 5. Comparison between the *frame rates* (fps) obtained by the various algorithms for holograms containing 256×256 , 512×512 , 768×768 , and 1024×1024 pixels. Vertical axis is logarithmic.

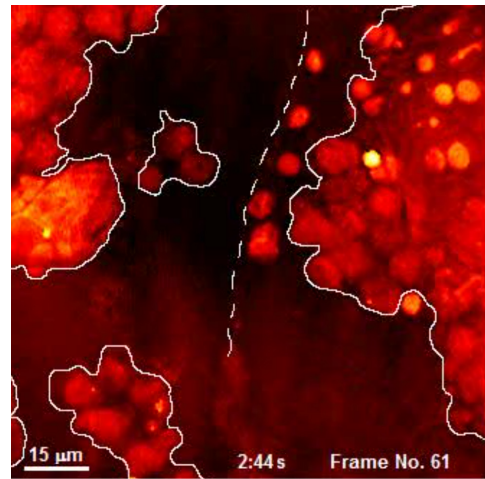


Fig. 6. Fast quantitative phase imaging of blood and epithelial cells flowing rapidly in a micro-channel, obtained by applying Algorithm C (see dynamics in Media 1).

frame rates, where 31.2 frames per second (fps), was obtained for 1 megapixel holograms, although modest and unparallelized computing was used.

To demonstrate using Algorithm C, we used it for real-time visualization of rapidly flowing blood and epithelial cells obtained from a wound (see Fig. 6 and Media 1). The cells flowed in a micro-channel created by two coverslips and clotted blood. In this case, the hologram contained 1024×1024 pixels, and the acquisition and processing was done in the full camera frame rate of 25 fps.

To conclude, we presented new and efficient algorithms that significantly increase the quantitative phase reconstruction frame rate, and enable more than video-rate processing for 1 megapixel holograms, allowing for real time visualization on a simple personal computer, with no parallel computing. Although sequential computing implementation was demonstrated, the presented algorithms can also obtain relative speedups on other computational platforms.

References

1. P. Girshovitz and N. T. Shaked, Biomed. Opt. Express **3**, 1757 (2012).
2. B. Kemper, P. Langehanenberg, and G. von Bally, Optik and Photonik **2**, 41 (2007).
3. H. Pham, H. Ding, N. Sobh, M. Do, S. Patel, and G. Popescu, Biomed. Opt. Express **2**, 1781 (2011).
4. T. Shimobaba, T. Ito, N. Masuda, Y. Ichihashi, and N. Takada, "Opt. Express **18**, 9955 (2010).
5. P. Girshovitz and N. T. Shaked, Light Sci. Appl. **3**, e151, in press (2014).
6. M. Paturzo, P. Memmolo, A. Tulino, A. Finizio, and P. Ferraro, Opt. Express **17**, 8709 (2009).
7. P. Girshovitz and N. T. Shaked, Opt. Express **21**, 5701 (2013).
8. M. A. Herráez, D. R. Burton, M. J. Lalor, and M. A. Gdeisat, App. Opt. **41**, 7437 (2002).

List of full references

1. P. Girshovitz and N. T. Shaked, "Generalized cell morphological parameters based on interferometric phase microscopy and their application to cell life cycle characterization," *Biomed. Opt. Express* **3**, 1757–1773 (2012).
2. B. Kemper, P. Langehanenberg, and G. von Bally, "Digital holographic microscopy: A new method for surface analysis and marker-free dynamic life cell imaging," *Optik and Photonik* **2**, 41–44 (2007).
3. H. Pham, H. Ding, N. Sobh, M. Do, S. Patel, and G. Popescu, "Off-axis quantitative phase imaging processing using CUDA: toward real-time applications," *Biomed. Opt. Express* **2**, 1781–1793 (2011).
4. T. Shimobaba, T. Ito, N. Masuda, Y. Ichihashi, and N. Takada, "Fast calculation of computer-generated-hologram on AMD HD5000 series GPU and OpenCL," *Opt. Express* **18**, 9955–9960 (2010).
5. P. Girshovitz and N. T. Shaked, "Doubling the field of view in off-axis low-coherence interferometric imaging," *Light Sci. Appl.* **3**, e151 (2014).
6. M. Paturzo, P. Memmolo, A. Tulino, A. Finizio, and P. Ferraro, "Investigation of angular multiplexing and de-multiplexing of digital holograms recorded in microscope configuration," *Opt. Express* **17**, 8709–8718 (2009).
7. P. Girshovitz and N. T. Shaked, "Compact and portable low-coherence interferometer with off-axis geometry for quantitative phase microscopy and nanoscopy," *Opt. Express* **21**, 5701–5714 (2013).
8. M. A. Herráez, D. R. Burton, M. J. Lalor, and M. A. Gdeisat, "Fast two-dimensional phase-unwrapping algorithm based on sorting by reliability following a noncontinuous path," *App. Opt.* **41**, 7437–7444 (2002).